

A Rare Thermally Induced Single Crystal to Single Crystal Transformation from a 2D Chiral Coordination Polymer to a 3D Chiral Coordination Polymer

Ping Zhu,^[a] Wen Gu,^[a] Li-Zhi Zhang,^[b] Xin Liu,^{*[a]} Jin-Lei Tian,^[a] and Shi-Ping Yan^[a]

Keywords: Crystal engineering / Coordination modes / Polymers

A rare single-crystal to single crystal (SCSC) transformation assisted by hydrogen bonding was induced thermally. A 2D homochiral coordination polymer $\{[\text{Ni}_2(\text{L-tar})_2(\text{H}_2\text{O})_2](\text{H}_2\text{O})_3\}_\infty$ was irreversibly converted into a 3D homochiral co-

ordination polymer, and the structure was confirmed by X-ray crystallography and XRD.

(© Wiley-VCH Verlag GmbH & Co. KGaA, 69451 Weinheim, Germany, 2008)

Introduction

Single crystal to single crystal (SCSC) transformations have received considerable interests in crystal engineering, because transition from one structure to another is difficult due to the restricted movements of molecules.^[1–5] Thus, numerous efforts have been employed to investigate SCSC transformations. SCSC transformations may be categorized into four main types according to the driving forces leading to the conversion: (a) Many SCSC transformations are caused by temperature changes. Several complexes demonstrate distinct crystal architectures under different temperatures with reversible transitions found.^[1] (b) Many SCSC transformations are induced by guest desorption/absorption, and several 3D complexes display shrinking or expanding to pursue optimal packing when they download/upload different guests.^[2] (c) Many SCSC transformations result from guest exchange. Several 2D complexes show sliding and many 3D complexes display shrinking or expanding to accommodate guests.^[3] (d) Many SCSC transformations are triggered by thermal treatment. The removal of bonded water creates coordination unsaturation in metal centers that can react topochemically with neighboring atoms.^[4] This type also includes thermally induced photopolymerization. Most of the reported polymerization cases involve the polymerization of unsaturated carbon bonds of ligands. It was reported recently that photo-induced electronic transfer can also trigger SCSC conversion.^[6] However thermally induced SCSC transitions are still very rare.^[4c,4f,4j–4l]

In this contribution, we report a rare thermally induced 2D–3D SCSC transition assisted by hydrogen bonding. It is also worthy to note that this SCSC transition involves formation of new covalent bonds, because just a few papers report that the single-crystalline nature of the coordination polymers is retained when structural transformations are accompanied with changes in the coordination environment of the metal ions.^[1a,2a,4c,4f,4j,4k] Such changes usually result in a loss of crystallinity.^[7] The 2D chiral $\{[\text{Ni}_2(\text{L-tar})_2(\text{H}_2\text{O})_2](\text{H}_2\text{O})_3\}_\infty$ (**1**; L-tar = L-tartarate) complex was previously reported,^[9] and we prepared it hydrothermally. Compound **1** crystallizes in the chiral orthorhombic space group $P2_12_12$. It was used to investigate SCSC transformation as well as dehydration/rehydration processes and their influence on the stacking mode,^[8] because it contains an extensive hydrogen-bonding network, through which the adjacent 2D layers are linked to a 3D supermolecule. After the dehydration of uncoordinated and coordinated water molecules to give the anhydrous $\{\text{Ni}(\text{L-tar})\}_\infty$ (**2**) form, remarkable changes in molecular arrangement occurred. The structure of compound **2** was determined by X-ray single-crystal diffraction, which revealed that it crystallizes in the chiral orthorhombic space group $I222$. The Flack parameters of two crystals are close to zero. The *b* and *c* axes in **1** correspond to the *c* and *b* axes in **2**, respectively. XRD tests of bulk **1** and **2** were performed, and they attest to their purity (Figure S1).

Results and Discussion

The dimeric entity of compound **1** is $\text{Ni}_2(\text{L-tar})_2(\text{H}_2\text{O})_2$, depicted in Figure 1a. Each Ni^{2+} ion is coordinated by two halves from two different tar ligands by chelating through the hydroxy oxygen atom (Ni2-O3) and the carboxyl oxygen atom (Ni2-O1). The octahedral configuration of the Ni^{2+} ion is supplemented by an aqua molecule (Ni2-O17w) and a nonchelating carboxyl oxygen atom of another dimer

[a] Department of Chemistry, Nankai University, Tianjin 300071, People's Republic of China
Fax: +86-22-23598473
E-mail: liuxin64@nankai.edu.cn

[b] School of Materials Science and Engineering, Nanyang Technological University, Singapore 639798, Singapore

Supporting information for this article is available on the WWW under <http://www.eurjic.org> or from the author.

(Ni2–O5^{#3}). Each dimer is linked to another four dimers to construct a corrugated 2D sheet through four links: carbonyl oxygen atoms O2, O5 in one tar ligand are bonded to two other Ni²⁺ ions and Ni1, Ni2 are bonded to two hydroxy O atoms O2^{#2}, O5^{#3} from two other dimers (Figure 3a). The Ni–O distances range from 2.0047(17) to 2.0960(18) Å, which are comparable to the reported values.^[9] Adjacent sheets are linked to a 3D supermolecule through H-bonds between coordinated water molecules and uncoordinated carboxyl oxygen atoms in an adjacent sheet (Figure S2).

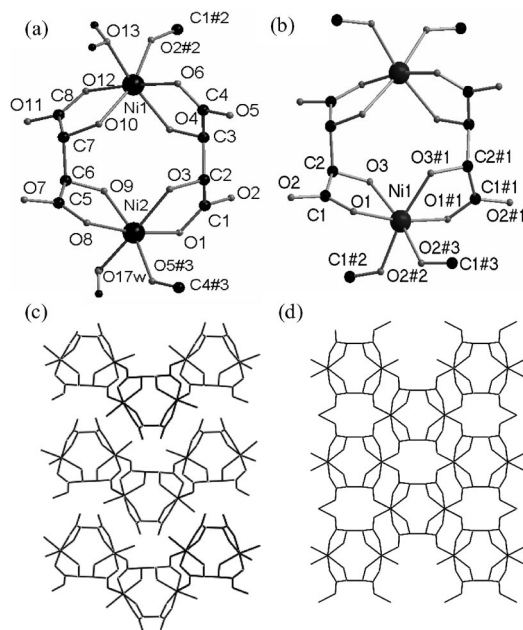


Figure 1. (a) Dimeric entity in **1**; (b) dimeric entity in **2**; (c) projections of the 2D sheet of **1** onto the *bc* plane; (d) projections of the 3D network of **2** onto the *bc* plane. Lattice water molecules and H atoms are omitted. Symmetry operations for **1**: #1: $x - 1/2, -y + 3/2, -z + 1$; #2: $-x, y + 1/2, -z + 1/2$; #3: $-x + 1, y - 1/2, -z + 1/2$; for **2** #1: $-x, -y + 2, z$; #2: $x - 1/2, -y + 3/2, -z + 1/2$; #3: $-x + 1/2, y + 1/2, -z + 1/2$. Selected bond length and angles are listed in Table S1.

Thermal gravimetric analysis (TGA) of **1** was performed under an N₂ atmosphere, and it shows loss of all water molecules in the range 83–150 °C (Figure S3). The number of water molecules removed (weight loss of 16.8%) corresponds to the theoretical calculation by using the empirical formula (17.8%, 5H₂O). As-synthesized crystalline solid **1** was dehydrated under vacuum at 150 °C overnight, which led to crystalline solid **2**. The thermal behavior of **1** is identical to that of **2** at temperatures higher than 150 °C (Figure S3).

To confirm the simultaneous structural transformation with the dehydration treatment and the thermal stability of **1**, variable-temperature X-ray powder diffraction (VT-XRPD) was recorded under vacuum in the temperature range 25–160 °C. Noticeable diffraction intensity variations in the XRD patterns of complex **1** were observed in this range, accompanied with position shifts of the Bragg peaks,

which can be ascribed to structural rearrangements following the departure of the water molecules (Figure 2). Upon heating, the pattern suddenly changed between 85 and 100 °C, which agrees with the TGA results. Attempts to rehydrate **2** to give **1** were unsuccessful; therefore, this SCSC conversion is irreversible.

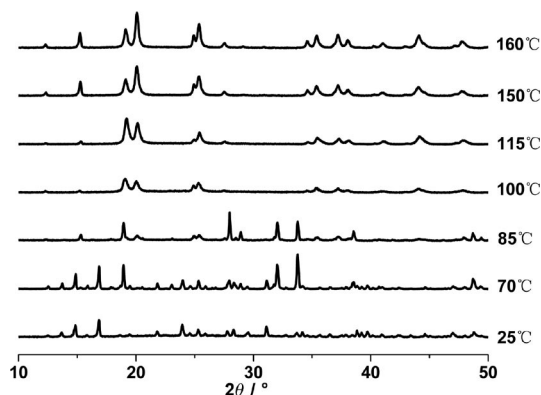


Figure 2. XRD patterns of compound **1** at variable temperatures.

In order to predict the transformed structure and analyze this process, it is useful to analyze H-bonds and geometric proximity.^[4e,4f,4j,4k] The hydrogen-bonded network in **1** provides favorable conditions for the SCSC process to take place (Figure S4). The geometric proximity of the carboxyl oxygen atoms and the Ni²⁺ ions appears to be beneficial for topochemical reactions to occur. The short Ni2B...O7 distance (4.080 Å) is maintained by the O–H17Bb...O7 (1.850 Å) hydrogen bond. The short Ni1...O11D distance (4.100 Å) is maintained by the O–H13a...O11D (1.850 Å) hydrogen bond (Figure 3a,b). When aqua molecules are removed, these carboxyl oxygen atoms are expected to bond to these Ni²⁺ ions owing to this topochemical geometry more than other neighboring Ni²⁺ ions. After the removal of coordinated waters, four new covalent bonds are formed: Ni2B–O7, Ni1–O11D, Ni1C–O11, and Ni2–O7A, the bond length of which is 2.038 Å, which is shorter than the distances (2.047 Å) between the Ni²⁺ ion and the carboxyl oxygen atoms in **1** (Figure 3c,d). Thus, a simple and sensible mechanism can be figured out. Aqua molecules are released by heat stimulus under vacuum. The removal of coordinated water molecules creates coordination unsaturation at the Ni²⁺ centers. They can be treated as Lewis acids. There are Lewis base uncoordinated carboxyl oxygen atoms in adjacent sheets, which react with the Lewis acids.

Although minimum movements of atoms and conformational changes can lead to this conversion, it is accompanied by a change in the space group from *P*2₁2₁2 to *I*222. The SCSC process leads to a higher density. A homochiral complex is supposed to demonstrate positive or negative Cotton effects in the CD spectra.^[10] In DMSO solution, sample **1** mainly displayed negative Cotton effects; sample **2** displayed notable negative Cotton effects (Figure S5).

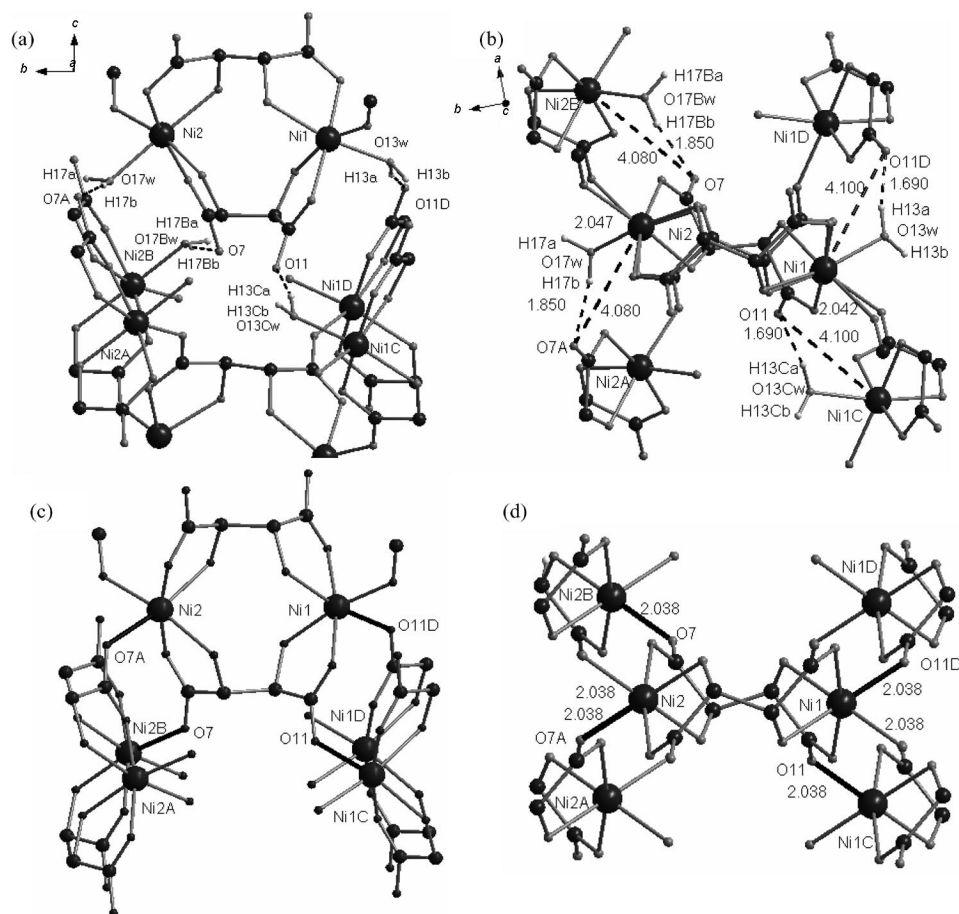


Figure 3. Schematic representation of the SCSC conversion of the units in **1** to form the 3D network in **2**: (a) and (b) geometric proximity and H-bond analysis; (c) view from the *a,c* direction before conversion; (d) view from the *a,c* direction after conversion. H-bonds are represented by dashes, with lengths indicated in (a) and (b). Distances between adjacent Ni and O atoms in (b) are also represented by dashes with lengths indicated; newly formed bonds are shown in (c) and (d). Uncoordinated water molecules are omitted. Distances [Å]: Ni2B...O7 4.080, Ni1...O11D 4.100, Ni1C...O11 4.080, Ni2...O7A 4.080; H-bonds [Å]: O–H17Bb...O7 1.850, O–H13a...O11D 1.850, O–H13Ca...O11 1.690, O–H14Bb...O7 1.690. Attention: marked atoms in (c) and (d) follow those in (a) and (b) for the sake of clarity, but these labels may differ from their true codes.

The dimeric entity of compound **2** is $[\text{Ni}_2(\text{L-tar})_2]$, which acts as a structural repeating unit (Figure 1b). The Ni^{2+} ion is chelated by two tar ligands in a *cis* orientation, with O1 from the carboxylate group and O3 from an adjacent OH group, and each tar ligand chelates the two metal centers in the dimer. The octahedra show rhombic distortion, with four Ni–O short distances [2.035(4)–2.038(4) Å] and two longer Ni–O distances [2.115(4) Å] in a *cis* orientation from the corresponding hydroxy oxygen atoms. Each dimer is linked to eight other dimers to form an infinite 3D polymer (Figure 2d) through the eight linkages (Figure S1b). The 2D sheet of **2** is formed on the *ac* plane in a similar way to that of **1**. A new Ni–O–C–O–Ni bridge in the *b* direction constructs the 3D framework.

Conclusions

This 2D–3D SCSC transition results from thermally induced polymerization of 2D homochiral networks into a 3D homochiral framework. To the best of our knowledge,

this is the first 2D–3D SCSC transition involving homochiral coordination polymers, which enriches the possibilities in crystal engineering. It is helpful to answer how we can build a convertible structure.

Experimental Section

1: A solution of $\text{Ni}(\text{OAc})_2$ (1 mmol 0.289 g) and L-tartaric acid (1 mmol, 0.150 g) in water (20 mL) was placed in a 25-mL Teflon-lined autoclave, sealed, and heated to 150 °C for 2 d, followed by cooling to 25 °C in air. The green crystals were filtered, washed with water and ethanol, and then dried in air. Yield: 65.7% (based on Ni). $\text{C}_8\text{H}_8\text{Ni}_2\text{O}_{17}$ (503.64): calcd. C 19.05, H 3.61; found C 18.75, H 3.87.

2: As-synthesized crystal **1** was dehydrated under vacuum at 150 °C overnight, which led to crystalline solid **2**. Yield: 100% (based on Ni). $\text{C}_8\text{H}_8\text{Ni}_2\text{O}_{12}$ (413.56): calcd. C 23.21, H 1.93; found C 23.03, H 2.00.

Single-Crystal Structure Determination: Measurements were carried out with a Bruker SMART 1000 CCD diffractometer with

Mo- K_{α} monochromated radiation ($\lambda = 0.71073 \text{ \AA}$) at 113(2) K. An empirical absorption correction was applied. The structures were solved by direct methods and refined by full-matrix least-squares against F^2 by using the SHELXS-97 and SHELXL-97 programs. Anisotropic thermal parameters were assigned to all non-hydrogen atoms. The hydrogen atoms were set in calculated positions and refined as riding atoms with a common fixed isotropic thermal parameter. Analytical expressions of neutral atom scattering factors were employed, and anomalous dispersion corrections were incorporated.

Crystal Data for 1: $\{[\text{Ni}_2(\text{L}-\text{C}_4\text{H}_4\text{O}_6)_2(\text{H}_2\text{O})_2]3\text{H}_2\text{O}\}_{\infty}$, $M = 2.157 \text{ Mg mol}^{-1}$, orthorhombic, space group $P2_12_12_1$, $a = 7.8141(8) \text{ \AA}$, $b = 11.0629(8) \text{ \AA}$, $c = 17.9430(14) \text{ \AA}$, $\alpha = \beta = \gamma = 90^\circ$, $V = 1551.1(2) \text{ \AA}^3$, $Z = 4$, $D_{\text{calcd.}} = 2.157 \text{ Mg m}^{-3}$, $T = 113(2) \text{ K}$, $m(\text{Mo}-K_{\alpha}) = 3.816 \text{ mm}^{-1}$, $-10 \leq h \leq 10$, $-14 \leq k \leq 14$, $-22 \leq l \leq 23$, $\text{GOF} = 1.008$, Flack parameters $0.016(10)$, $wR_2 = 0.0510$ (for 813 independent reflections [$R_1 = 0.0328$]), $R_1 = 0.0286$ [$I > 2\sigma(I)$].

Crystal Data for 2: $\{\text{Ni}(\text{L}-\text{C}_4\text{H}_4\text{O}_6)\}_{\infty}$, $M = 2.658 \text{ Mg mol}^{-1}$, orthorhombic, space group $I222$, $a = 4.9740(11) \text{ \AA}$, $b = 9.055(2) \text{ \AA}$, $c = 11.472(2) \text{ \AA}$, $\alpha = \beta = \gamma = 90^\circ$, $V = 516.68(19) \text{ \AA}^3$, $Z = 8$, $D_{\text{calcd.}} = 2.658 \text{ Mg m}^{-3}$, $T = 113(2) \text{ K}$, $m(\text{Mo}-K_{\alpha}) = 3.816 \text{ mm}^{-1}$, $-5 \leq h \leq 5$, $-10 \leq k \leq 10$, $-13 \leq l \leq 13$, $\text{GOF} = 1.121$, Flack parameters $-0.01(6)$, $wR_2 = 0.0935$ (for 813 independent reflections [$R_1 = 0.0392$]), $R_1 = 0.0384$ [$I > 2\sigma(I)$].

CCDC-634956 (for **1**) and -650895 (for **2**) contain the supplementary crystallographic data for this paper. These data can be obtained free of charge from The Cambridge Crystallographic Data Centre via www.ccdc.cam.ac.uk/data_request/cif.

Supporting Information (see footnote on the first page of this article): Additional figures, selected bond length and angles, and TGA analysis

Acknowledgments

This work was supported by the National Natural Science Foundation of China (Grant 20371027 and 20771062)

- [1] a) C. Hu, U. Englert, *Angew. Chem. Int. Ed.* **2005**, *44*, 2281–2283; b) -P. Ma, Y.-B. Dong, R.-Q. Huang, M. D. Smith, C.-Y. Su, *Inorg. Chem.* **2005**, *44*, 6143–6145; c) J.-P. Zhang, Y.-Y. Lin, W.-X. Zhang, X. M. Chen, *J. Am. Chem. Soc.* **2005**, *127*, 14162–14163; d) Y.-M. Legrand, A. van der Lee, N. Masquelez, P. Rabu, M. Barboiu, *Inorg. Chem.* **2007**, *46*, 9083–9089.

- [2] a) C.-L. Chen, A. M. Goforth, M. D. Smith, C.-Y. Su, H.-C. zur Loye, *Angew. Chem. Int. Ed.* **2005**, *44*, 6673–6677; b) G. J. Halder, C. J. Kepert, *J. Am. Chem. Soc.* **2005**, *127*, 7891–7900; c) X.-M. Zhang, Z.-M. Hao, W.-X. Zhang, X.-M. Chen, *Angew. Chem. Int. Ed.* **2007**, *46*, 3456–3459.
- [3] a) K. Takaoka, M. Kawano, M. Tominaga, M. Fujita, *Angew. Chem. Int. Ed.* **2005**, *44*, 2151–2154; b) O. Ohmori, M. Kawano, M. Fujita, *J. Am. Chem. Soc.* **2004**, *126*, 16292–16293; c) C.-D. Wu, W. Lin, *Angew. Chem. Int. Ed.* **2005**, *44*, 1958–1961; d) M. Nihei, L. Han, H. Oshio, *J. Am. Chem. Soc.* **2007**, *129*, 5312–5313.
- [4] a) M. Nagarathinam, J. J. Vittal, *Angew. Chem. Int. Ed.* **2006**, *45*, 4337–4341; b) E. Ruiz-Agudo, S. Galli, J. A. R. Navarro, *Inorg. Chim. Acta* **2007**, *360*, 84–90; c) A. K. Sah, T. Tanase, *Chem. Commun.* **2005**, 5980–5981; d) C. Hu, U. Englert, *Angew. Chem. Int. Ed.* **2006**, *45*, 3457–3459; e) J. D. Ranford, J. J. Vittal, D. Wu, *Angew. Chem. Int. Ed.* **1998**, *37*, 1114–1116; f) J. D. Ranford, J. J. Vittal, D. Wu, X. Yang, *Angew. Chem. Int. Ed.* **1999**, *38*, 3498–3501; g) V. Niel, A. L. Thompson, M. C. Muoz, A. Galet, A. E. Goeta, J. A. Real, *Angew. Chem. Int. Ed.* **2003**, *42*, 3760–3763; h) B. Rather, M. J. Zaworotko, *Chem. Commun.* **2003**, 830–831; i) W. Kaneko, M. Ohba, S. Kitagawa, *J. Am. Chem. Soc.* **2007**, *129*, 13706–13712; j) X.-N. Cheng, W.-X. Zhang, X.-M. Chen, *J. Am. Chem. Soc.* **2007**, *129*, 15738–15739; k) D.-X. Xue, W.-X. Zhang, X.-M. Chen, H.-Z. Wang, *Chem. Commun.* **2008**, 1551–1553; l) J. Ye, Y. Liu, Y. Zhao, X. Mu, P. Zhang, Y. Wang, *CrystEngComm* **2008**, 598–604.
- [5] a) J. J. Vittal, *Coord. Chem. Reviews.* **2007**, *251*, 1781–1795; b) S. Kitagawa, K. Uemura, *Chem. Soc. Rev.* **2005**, *34*, 109–119.
- [6] L.-Z. Zhang, W. Gu, X. Liu, Z.-L. Dong, B. Li, *CrystEngComm*, DOI: 10.1039/b718523e.
- [7] a) N. Yanai, W. Kaneko, K. Yoneda, M. Ohba, S. Kitagawa, *J. Am. Chem. Soc.* **2007**, *129*, 3496–3497; b) R. Sun, Y.-Z. Li, J. Bai, Y. Pan, *Cryst. Growth Des.* **2007**, *7*, 890–894; c) X.-L. Hong, Y.-Z. Li, H. Hu, Y. Pan, J. Bai, X.-Z. You, *Cryst. Growth Des.* **2006**, *6*, 1221–1226.
- [8] a) K. Uemura, K. Saito, S. Kitagawa, H. Kita, *J. Am. Chem. Soc.* **2006**, *128*, 16122–16130; b) X.-N. Cheng, W.-X. Zhang, Y.-Y. Lin, Y.-Z. Zheng, X.-M. Chen, *Adv. Mater.* **2007**, *19*, 1494–1498.
- [9] a) L. J. Bostelaar, R. A. G. De Graaff, F. B. Hulsbergen, J. Reedijk, W. M. H. Sachtler, *Inorg. Chem.* **1984**, *23*, 2294–2297; b) S. Scherb, C. NaËther, W. Bensch, *Acta Crystallogr., Sect. C* **2002**, *58*, m135–m136.
- [10] a) G. L. J. Rikken, E. Raupach, *Nature* **1997**, *390*, 493–494; b) S. Thushari, J. A. K. Cha, H. H.-Y. Sung, S. S.-Y. Chui, A. L.-F. Leung, Y.-F. Yen, I. D. Williams, *Chem. Commun.* **2005**, 5515–5517.

Received: March 16, 2008
Published Online: May 28, 2008